

Spatial profiling of the tumor microenvironment in head and neck cancer identifies immune checkpoints and proteins involved in cell death signaling biomarkers of immunotherapy response



Disclaimer: All Visiopharm products in this poster are intended for research use only (RUO).

Habib Sadeghirad¹, Ning Liu², James Monkman¹, Chin Wee Tan², Caroline Cooper³, Jeni Caldara⁵, Brenna O'Neill⁵, Sarah E. Church⁴, Kyla Teplitz⁴, Kara Gorman⁴, Fabian Schneider⁵, James Mansfield⁵, Ken O'Byrne³, Melissa Davis², Brett Hughes⁶, Arutha Kulasinghe^{1*}

1 – The University of Queensland, Brisbane, Australia; 2 – The Walter and Eliza Hall Institute (WEHI), Melbourne, Australia; 3 – The Princess Alexandra Hospital, Brisbane, Australia; 4 – NanoString Technologies, Seattle, WA, USA; 5 – Visiopharm, Horsholm, Denmark; 6 – The Royal Brisbane and Women's Hospital, Brisbane, Australia; *arutha.kulasinghe@uq.edu.au

Background and Methods

Immune checkpoint inhibitors (ICIs) Pembrolizumab and Nivolumab have shown promising results in patients with recurrent or metastatic (R/M) head and neck squamous cell carcinoma (HNSCC). Nonetheless, only up to 20% of patients may benefit from them. Next generation predictive biomarkers of response to ICI therapies are currently needed.

This retrospective study profiled pre-treatment tissue samples collected from R/M HNSCC patients (n=30) treated with Pembrolizumab or Nivolumab. Targeted spatial proteomics profiling was performed using NanoString's GeoMx® Digital Spatial Profiler (GeoMx). To develop an informed region-of-interest (ROI) selection strategy for the GeoMx, we analyzed H&E images from serial sections and performed Oncotopix® Discovery software analysis, which considered pathology inputs and machine learning to analyze H&E imagery and 3-channel GeoMx visualization inputs. We profiled 80 proteins simultaneously using the GeoMx across modules in cell death, immune activation, immune cell typing, immuno-oncology drug target, immune profiling, PI3K/AKT signaling, and pan-tumor markers. Next, we performed differential expression (DE) analysis of the proteins localized in the tumor and stromal compartments against response to therapy parameters of complete, partial, stable and progressive disease (according to RECIST criteria). Three-channel GeoMx immunofluorescence images provided per-ROI cell counts (total and phenotyped based on 2 markers), and these data were used to aid in area and cell count normalization within the tumor and stromal compartments.

Data Collection

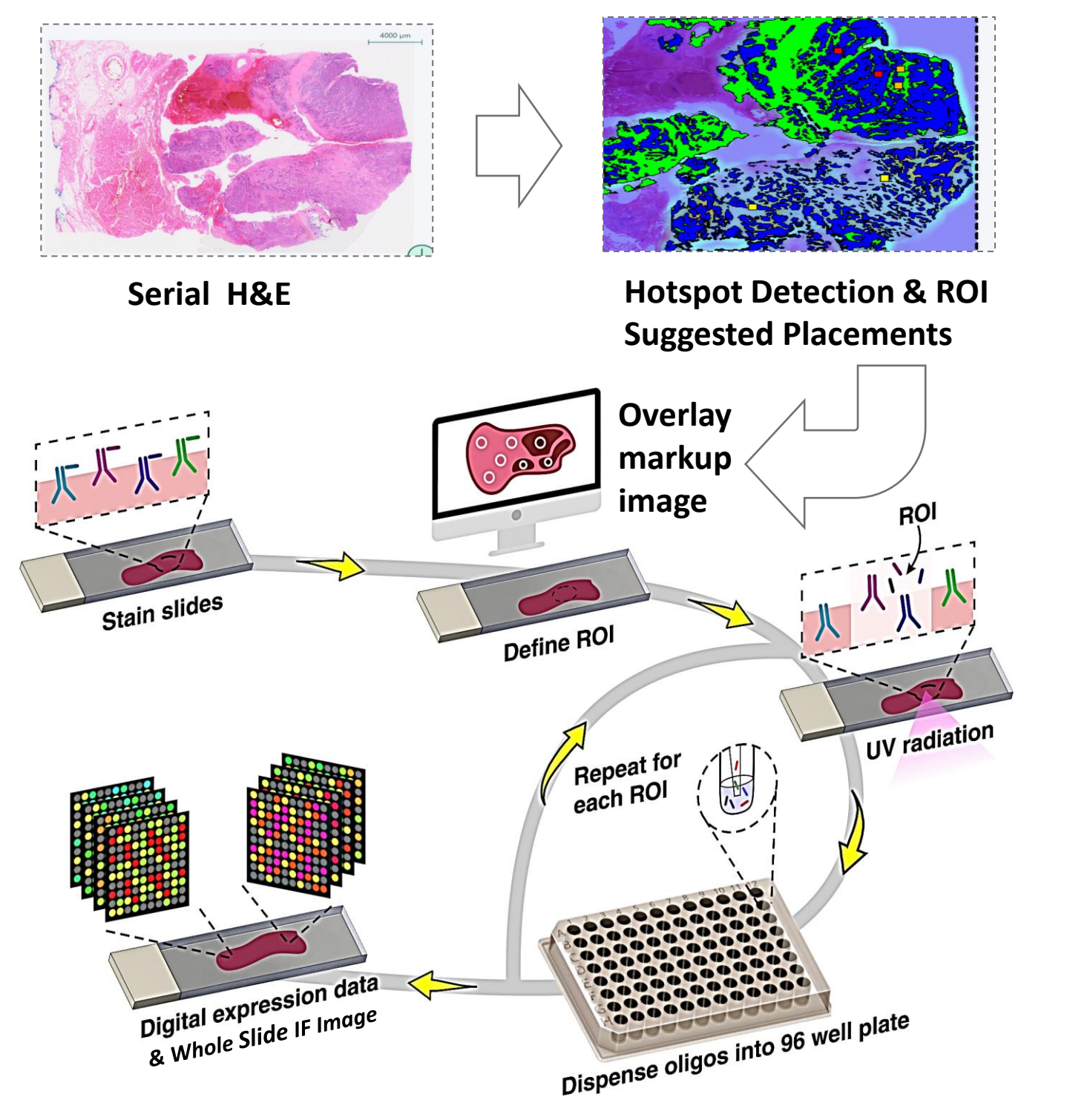


Figure 1: ROI selection and GeoMx data collection. GeoMx ROI selection was performed using Oncotopix® Discovery software. Whole-slide H&E images were analyzed using a pre-existing APP for lymph node metastasis detection and 6 ROIs were selected based on low, middle and high amounts of tumor. Selected ROIs were used for standard GeoMx protein data collection.

Downstream Image Analysis

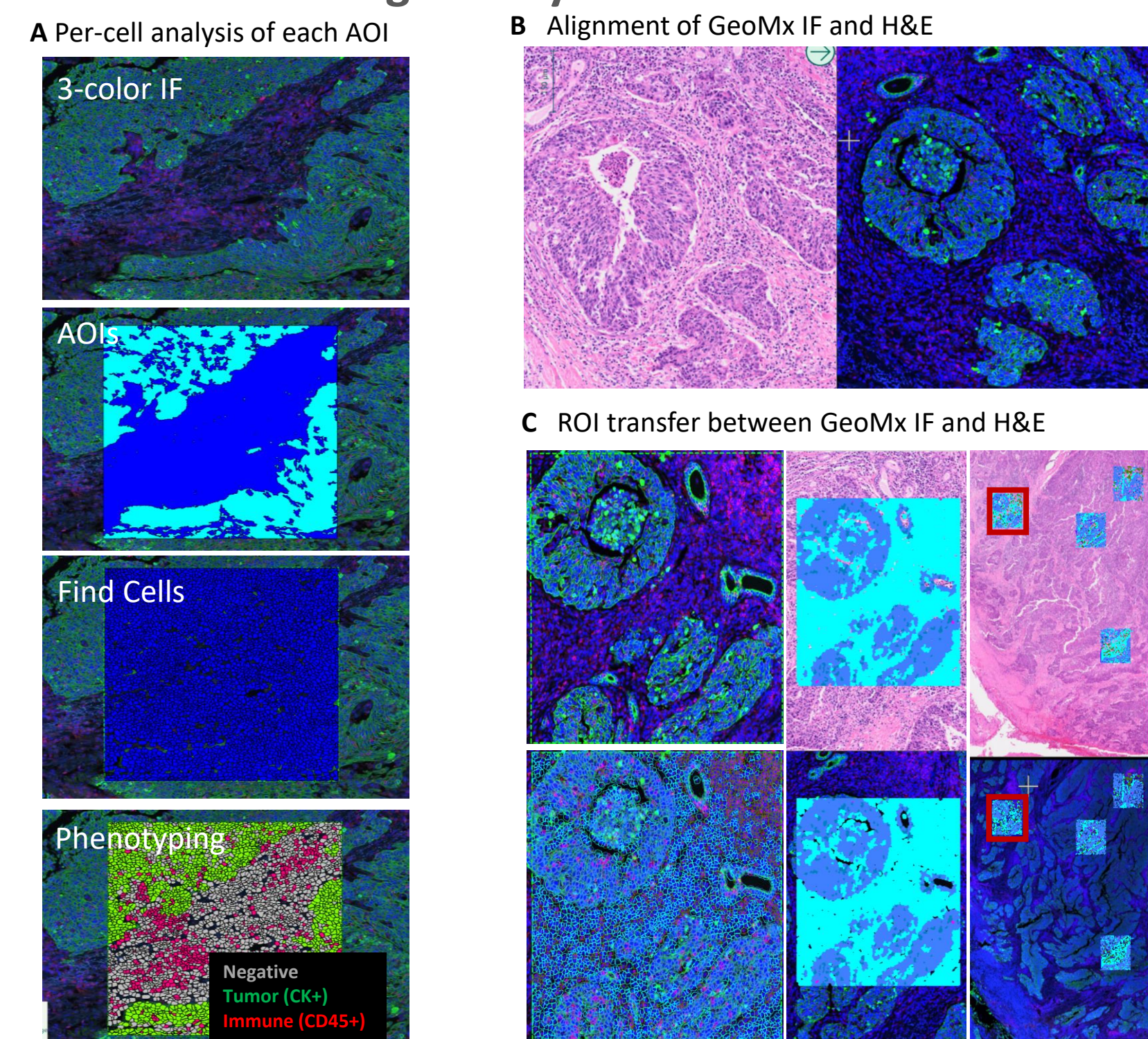


Figure 2 Image analysis. A. For two patients, the 3-channel GeoMx IF images (FITC, nuclei, blue; Cy3, cytokeratin, green; Texas Red, CD45, red) and the regions of interest (ROIs) and areas of illumination (AOIs) from which the protein signatures were acquired (6 ROIs per slide) were imported into Oncotopix® Discovery. Within each ROI, one AOI was acquired using a cytokeratin mask ('tumor') and another AOI for the rest of the ROI ('stroma'). Each AOI mask was analyzed for tissue area, cell number, and phenotype (Figure 3 below). B. 40x whole-slide H&E serial section images were aligned with their corresponding GeoMx 20x IF images using Tissuealign™. C. GeoMx ROIs were then transferred to the H&E image for further analysis of the same regions. Whole slide analysis was also performed. Note: The two images are not to the same scale.

Per-AOI Image Cell Counts Correlation with GeoMx Protein

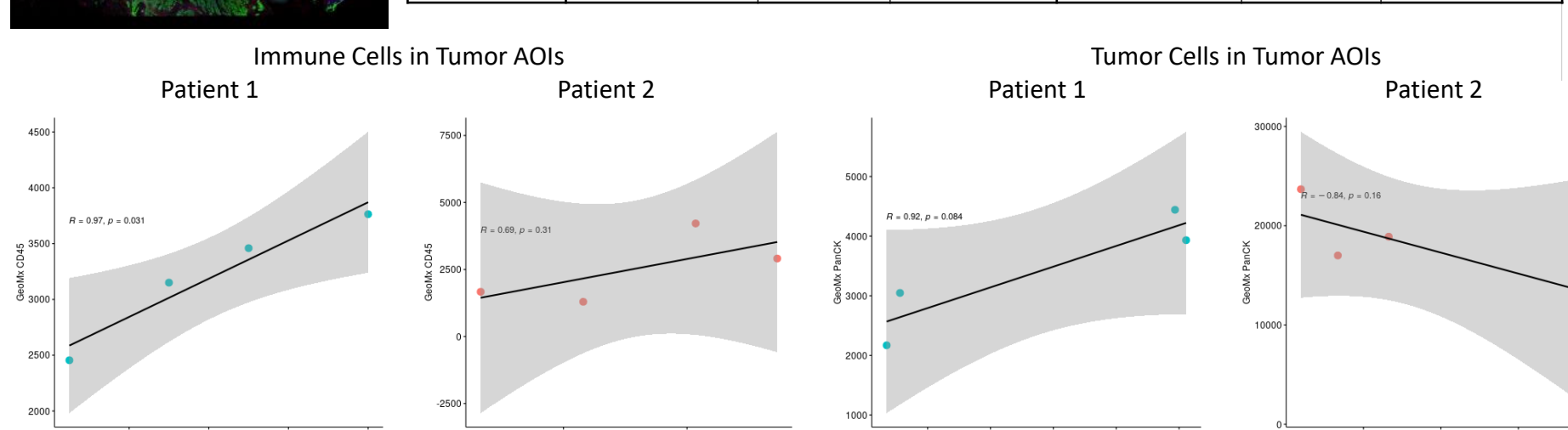
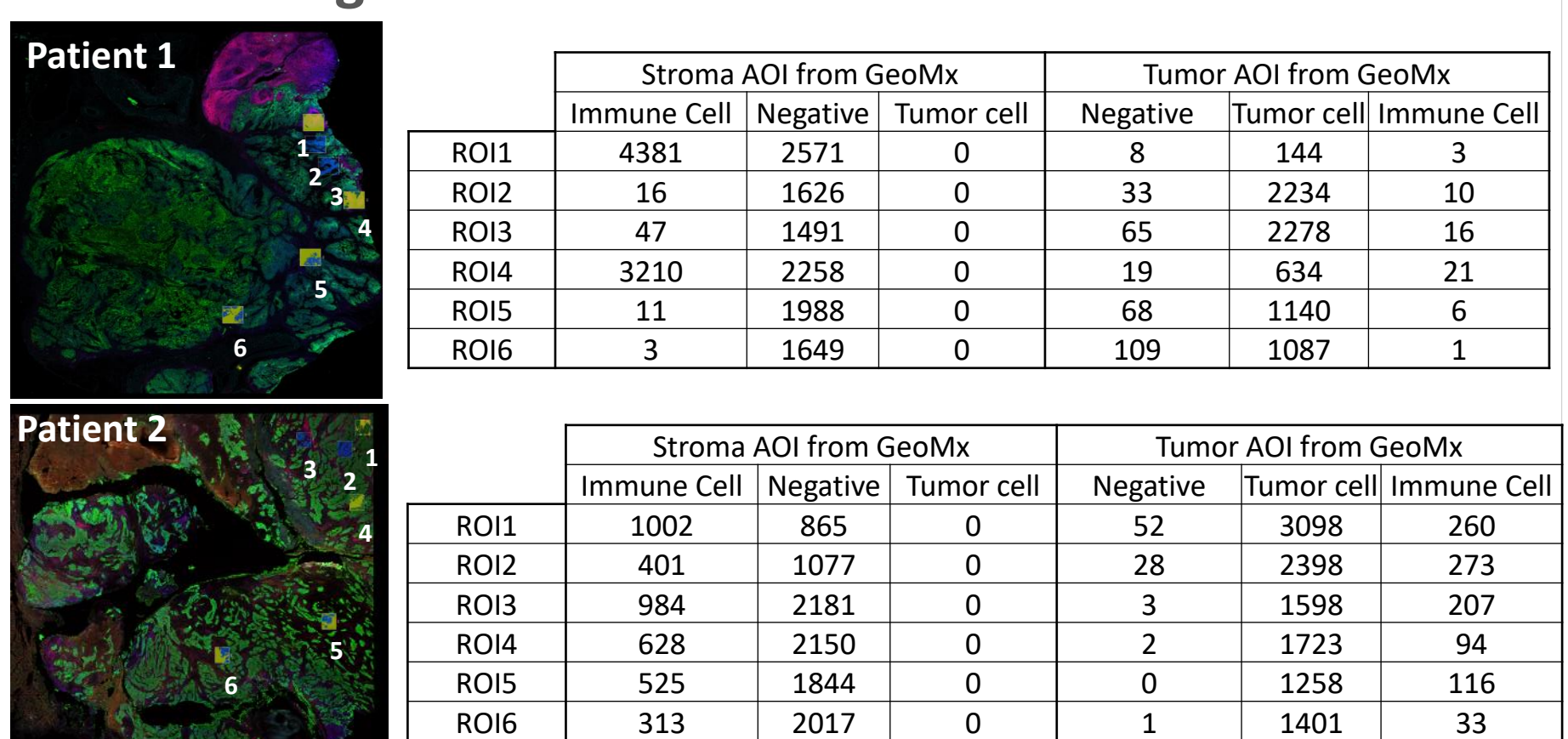


Figure 3. For 2 patients each of the 6 ROIs were phenotyped and counted for immune, tumor and negative cells in both the Stroma and Tumor areas. GeoMx protein counts for CD45 (all immune cells) and PanCK (tumor cells) in tumor segments were correlated between the counted cell phenotypes per patient.

Results

Differential Expression of Profiled Proteins

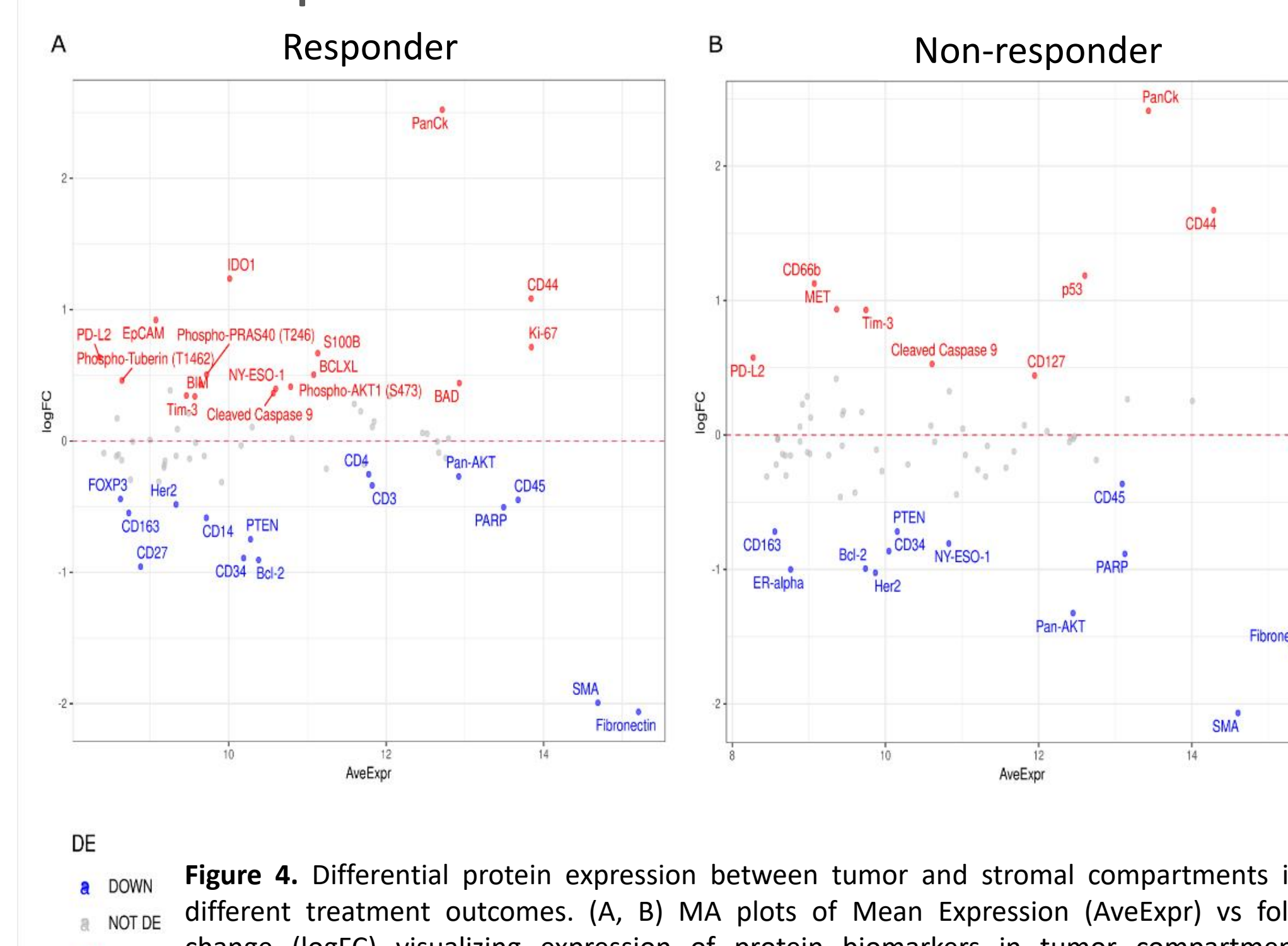


Figure 4. Differential protein expression between tumor and stromal compartments in different treatment outcomes. (A, B) MA plots of Mean Expression (AveExpr) vs fold change (logFC) visualizing expression of protein biomarkers in tumor compartment compared to stromal compartments in (A) Responders or (B) non-responders. Colors denote not differentially expressed markers (gray), significantly up- (red) and down-regulated (blue) markers based on false discovery rate (FDR) < 0.05 after multiple comparison testing.

Survival Analysis

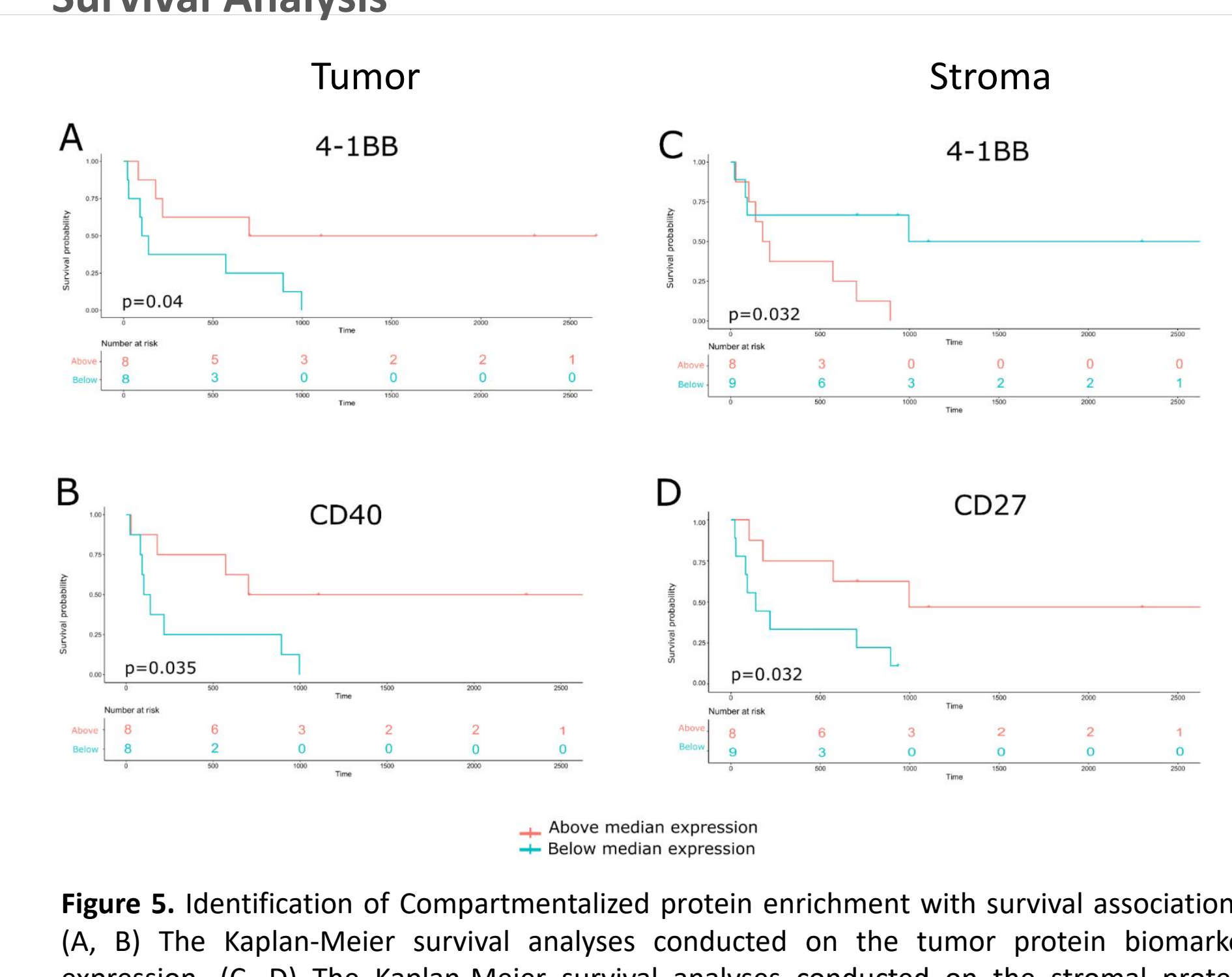


Figure 5. Identification of Compartmentalized protein enrichment with survival associations. (A, B) The Kaplan-Meier survival analyses conducted on the tumor protein biomarker expression. (C, D) The Kaplan-Meier survival analyses conducted on the stromal protein biomarker expression. The p-value of the curves is calculated using the log-rank test.

Cell Composition by Image Analysis

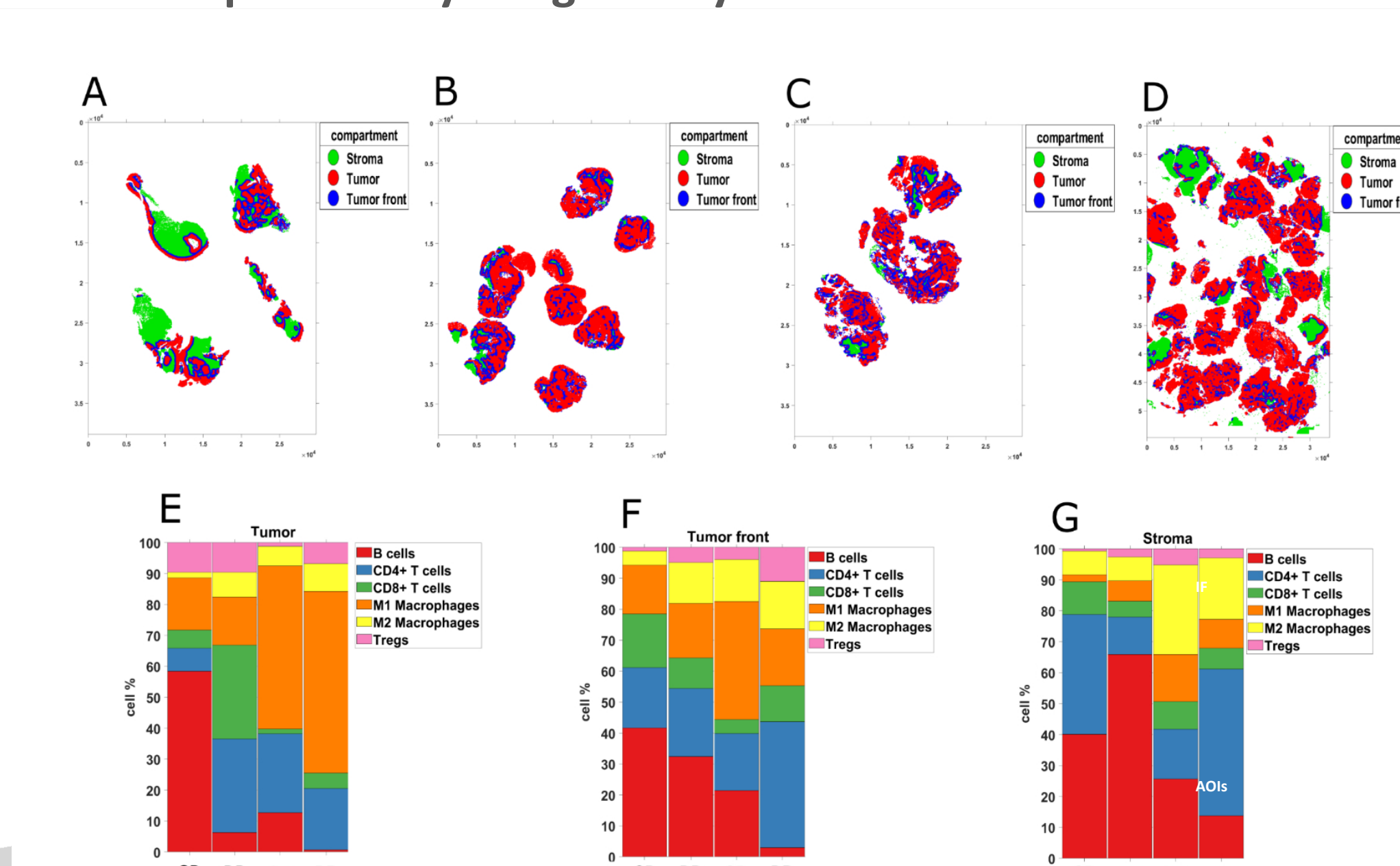


Figure 6. Compartmentalized analysis. (A-D) Tissue segmentation of patients with CR, PR, SD, and PD, from left to right respectively. (E-G) The bar chart representing Compartmentalized cell type composition across tissue samples from patients with CR, PR, SD, and PD, from left to right.

Discussion

Here we show integration of two complementary platforms to interrogate cell phenotypes and deep characterization of the tumor microenvironment in response to therapy. We were able to investigate heterogeneity within tumors and amongst different patient's tumors by both digital phenotyping and deep proteomic analysis. This is exemplified by the immune and tumor cell phenotyping and protein count correlations, where immune cells counts between the two platforms were highly correlated but tumor cell and pan-cytokeratin expression was only correlated in one sample. This could be due to intrinsic differences in the epithelial tumor cells and supports this workflow as a tool to discover important biology and biomarkers that are related to the tumor microenvironment.

Conclusion

We found that patients responsive to immunotherapy had higher expression levels of PD-L1, Bcl-2, BCLX, and CD68 in the tumor, whereas VISTA, FOXP3, and CD66b were downregulated. In the stromal compartment, it was found that responders had higher expression levels of B7-H3, CD40, and SMA, but lower expression of PARP, S100B, and NY-ESO-1 in comparison to non-responders. In terms of best response analysis, patients with PR (n=5) had higher levels of PD-L1, ER-alpha, and CD68 expression, but lower levels of VISTA, CD27, and CD95/Fas in tumor regions than patients with PD (n=8). In the stroma, PD-L1, CD68, and HLA-DR were upregulated, while VISTA, BIM, and BAD were downregulated in patients with PR versus those with PD.

The informed ROI selection strategy aided in defining key features in the tumor microenvironment for comparative analysis across samples, and for data normalization methods. Moreover, we found that immune checkpoints and proteins involved in cell death signaling play important roles in the immune responsive tumor microenvironment of HNSCC based on response to immunotherapy.

Better predictive biomarkers of response to immunotherapy are currently needed for Head and Neck Cancers. This study demonstrated informed 'Region of Interest (ROI)' capture using the Oncotopix Discovery to analyze whole slides to demarcate tumour/stroma and gross tissue and cellular structures upstream of ROI selection on H&E. Absolute counts for cell types in the tumour and stroma were obtained for quantification and comparison with the GeoMx DSP results. Tumour and stromal compartment specific protein profiles were obtained which associated with response to therapy metrics. Validation of these findings is currently ongoing.